Anal. Chem. **2003,** *75,* 2959−2966

Articles

Scanning Electrochemical Microscopy. 46. Shielding Effects on Reversible and Quasireversible Reactions

Cynthia G. Zoski,*,† Julio C. Aguilar,‡ and Allen J. Bard*,‡

Department of Chemistry and Biochemistry, The University of Texas at Austin, Austin, Texas 78712, and Chemistry Department, Georgia State University, Atlanta, Georgia 30303

An approximate theory for the feedback mode of the scanning electrochemical microscope (SECM) is developed to interpret the effects of substrate shielding on an ultramicroelectrode tip during a recording of i_T versus d curves (approach curves) for reversible and quasireversible kinetics at a substrate surface. The resulting expressions for the tip current, i_T, show a good fit to more accurate SECM simulations as well as to the experimental response of a reversible and quasireversible reaction. SECM shielding experiments thus give an interesting new insight into SECM approach curves over electrodes at different potentials, which suggest possible applications to measuring heterogeneous kinetics for fast reactions and diffusion coefficient determination.

Quantitative studies with the scanning electrochemical microscope (SECM) are usually based on measurements of the tip current, i_T, as a function of the tip−substrate separation, d.[1−10] These i_T versus d, or approach, curves can be used, for example, to identify conductive zones on a substrate, where diffusion-controlled positive feedback is observed and i_T increases with decreasing d. Thus, if an oxidizing species is reduced at the tip ($O + ne \rightarrow R$) and the substrate is at a sufficiently positive potential, the tip-generated R is oxidized back to O at the substrate. At insulating zones on the substrate, no oxidation of R occurs and the approach curve is characterized as showing negative feedback (i_T decreases as d decreases).

Approach curves can also be used to measure heterogeneous electron-transfer kinetics at the substrate surface.[10−13] For example, in studying electrocatalysis at a substrate electrode, the tip is held at a potential where the $O \rightarrow R$ reaction is diffusion controlled, and approach curves are taken at different substrate potentials, E_S. Generally, E_S is controlled so that the process at the substrate ($R \rightarrow O$) is always opposite to that at the tip ($O \rightarrow R$). However, one can also operate at E_S values where, for at least part of the approach curve, the same process ($O \rightarrow R$) occurs at both substrate and tip. In this case, the substrate "shields" the tip, so that i_T will decrease below the value found over an insulator. Even under shielding conditions, as we show in this paper, the reaction at the substrate can change from $O \rightarrow R$ to $R \rightarrow O$ as the tip approaches the substrate.

The nature of the response under shielding conditions depends on the extent of interaction of the diffusion layers of the tip and substrate and can be divided into three zones (Figure 1). At large d (Figure 1A), there is no interaction between tip and substrate, and $i_T = i_{T,\infty}$, the value of the tip current in the bulk solution. At intermediate d (Figure 1B), the tip senses a decreasing concentration of O as it moves into the substrate diffusion layer. At very small d (Figure 1C), the tip diffusion layer interacts with the small portion of the substrate beneath the tip. In this last region, the concentration profiles near the substrate are perturbed and it is possible to see positive feedback, even when the substrate potential is set so that the overall reaction is still $O \rightarrow R$.

The shielding that is seen with the SECM is analogous to that found with other two-electrode electrochemical systems, such as the rotating ring−disk electrode (RRDE) or interdigitated electrodes. For example, with the RRDE, the current at the ring electrode decreases when the disk is placed at a potential where the same reaction is occurring.[14,15] However, because the convec-

* Corresponding author. E-mail: checgz@panther.gsu.edu.
† Georgia State University.
‡ The University of Texas at Austin.

(1) Bard, A. J.; Fan, F.-R. F.; Pierce, D. T.; Unwin, P. R.; Wipf, D. O.; Zhou, F. *Science* **1991**, *254*, 68.
(2) Bard, A. J.; Fan, F.-R. F.; Mirkin, M. V. In *Electroanalytical Chemistry*; Bard, A. J., Ed.; Dekker: New York, 1994; Vol. 18, p 243.
(3) Arca, M.; Bard, A. J.; Horrocks, B. R.; Richards, T. C.; Treichel, D. A. *Analyst* **1994**, *119*, 719.
(4) Mirkin, M. V. *Mikrochim. Acta* **1999**, *130*, 127.
(5) Bard, A. J.; Fan, F.-R. F.; Mirkin, M. V. In *Handbook of Surface Imaging and Visualization*; Hubbard, A. T., Ed.; CRC: Boca Raton, FL, 1995; p 667.
(6) Bard, A. J.; Fan, F.-R. F.; Mirkin, M. V. In *Physical Electrochemistry: Principles, Methods and Applications*; Rubenstein, I., Ed.; Marcel Dekker: New York, 1995; p 209.
(7) Engstrom, R. C.; Weber, M.; Wunder, D. J.; Burgess, R.; Winquist, S. *Anal. Chem.* **1986**, *58*, 844.
(8) Engstrom, R. C.; Meaney, T.; Tople, R.; Wightman, R. M. *Anal. Chem.* **1987**, *59*, 2005.
(9) Engstrom, R. C.; Wightman, R. M.; Kristensen, E. W. *Anal. Chem.* **1988**, *60*, 652.
(10) *Scanning Electrochemical Microscopy*; Bard, A. J., Mirkin, M. V., Eds.; Marcel Dekker: New York, 2001.
(11) Wipf, D. O.; Bard, A. J. *J. Electrochem. Soc.* **1991**, *138*, L4.
(12) Bard, A. J.; Mirkin, M. V.; Unwin, P. R.; Wipf, D. O. *J. Phys. Chem.* **1992**, *96*, 1861.
(13) Engstrom, R. C.; Small, B.; Kattan, L. *Anal. Chem.* **1992**, *64*, 241.
(14) Bard, A. J.; Faulkner, L. R. *Electrochemical Methods*; Wiley: New York, 2001; p 352.

10.1021/ac034011x CCC: $25.00
Published on Web 05/17/2003

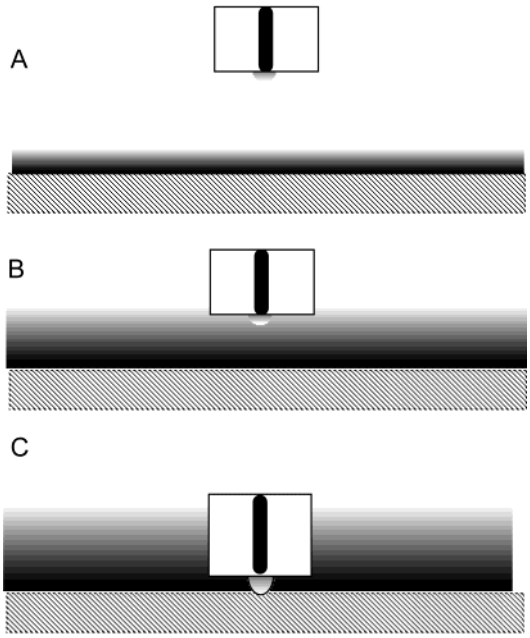

Figure 1. Schematic diagram of tip and substrate diffusion layers at different separations, d: (A) no interaction; (B) tip enters substrate diffusion layer; (C) substrate senses tip diffusion layer.

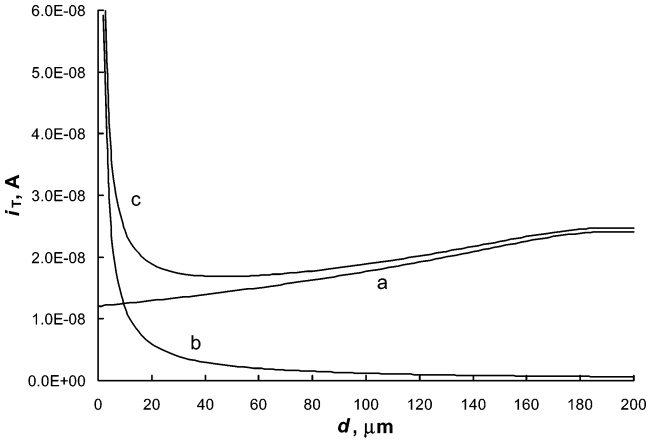

Figure 2. Calculated approach curves: (a) shielding alone (eq 6); (b) feedback alone (thin-layer approximation) (eq 11); (c) overall (sum of a and b). Calculated for $\theta = 1$ (half-wave potential) for $a = 12.5$ μm, $n = 1$, $C_O^* = 10$ mM, $D = 5 \times 10^{-6}$ cm^2/s, $\tau = 1$ s, $d_i = 200$ μm, and $\mu = 4$ μm/s.

tive flow is totally from disk to ring (ring collection), one never sees a transition to the equivalent of SECM positive feedback. Shielding is also found with IDAs,[16] where feedback is possible. Shielding experiments of the type described here have not been carried out, to our knowledge.

THEORY

While it would be possible to do a detailed simulation of the approach curves, as carried out for example in studies of heterogeneous kinetics,[12] we treat the problem here in a more approximate way that makes the quantitative behavior more transparent. Moreover, as shown below, the resulting expressions for i_T fit more accurate simulations and the experimental response quite well. We first treat a Nernstian system and then a more general system involving quasireversible electron transfer at the substrate, which, in all cases, is assumed to have a much larger area than the tip electrode. We consider the case for a reduction reaction at the tip

$$O + ne \rightarrow R \qquad (1)$$

with the tip potential, E_T, held at sufficiently negative value that reduction of O is diffusion controlled.

Nernstian Systems. We assume that the tip is initially at a distance, d_i, from the substrate (at $x = 0$) and it is held there for a quiet time, τ, during which a potential is applied to both tip and substrate. During this time, if E_S is set so that reaction 1 occurs, a concentration gradient forms near the substrate. At time, τ, the tip begins a scan toward the substrate at a scan rate, μ. At E_S, the concentration ratio at the substrate surface is given by the Nernst equation[17]

$$C_O(0,t)/C_R(0,t) = \theta = \exp[(nF/RT)(E - E^{\circ\prime})] \qquad (2)$$

The concentration profile that forms at the substrate, assuming that linear diffusion at the substrate occurs, is given by[17]

$$C_O(x,t) = \frac{C_O^*}{(1+\xi\theta)}\left\{\mathrm{erf}\left[\frac{x}{2(D_O t)^{1/2}}\right] + \xi\theta\right\} \qquad (3)$$

where $\xi = (D_O/D_R)^{1/2}$ and C_O^* is the bulk concentration of O. The tip samples this concentration gradient when it is at a distance $x = d$. The time to reach that point is

$$t = \tau + [(d_i - d)/\mu] \qquad (4)$$

so that $C_O(d)$ is given by

$$C_O(d) = \frac{C_O^*}{(1+\xi\theta)}\left\{\mathrm{erf}\left[\frac{d}{2\{D_O[\tau + (d_i - d)/\mu]\}^{1/2}}\right] + \xi\theta\right\} \qquad (5)$$

Within this zone, shown in Figure 1A and B, i_T is given by

$$i_T = 4nFD_O a C_O(d) \qquad (6)$$

An approach curve in this region for $\theta = 1$ (corresponding to $E = E^{\circ\prime}$) is shown in Figure 2a.

However, when the tip gets sufficiently close to the substrate, the tip concentration profile perturbs that small part of the substrate beneath the tip, and this sets up the possibility of positive feedback. This arises because the concentrations near the substrate surface are no longer controlled by diffusion from the

(15) Albery, W. J.; Hitchman, M. L. *Ring-Disc Electrodes*; Clarendon: Oxford, 1971; p 24.
(16) Bard, A. J.; Crayston, J. A.; Kittlesen, G. P.; Varco Shea, T.; Wrighton, M. S. *Anal. Chem.* **1986**, *58*, 2321.
(17) Bard, A. J.; Faulkner, L. R. *Electrochemical Methods*; Wiley: New York, 2001; pp 177, 179.

surface. This can be treated approximately by considering the tip and substrate as forming a two-electrode thin-layer cell, as has been used in previous work on SECM.[18,19] This follows the previous treatments of such cells,[20−22] where the concentrations of species at the two electrode surfaces (tip and substrate) are determined by the potentials of the electrodes, E_T and E_S, and a steady state is assumed. In this case, assuming $D_O = D_R = D$, and that E_T is at a potential where the reduction of O is mass-transfer controlled

$$i_T = \frac{nFADC_{O,S}}{d} = \frac{nFAD(C_{R,T} - C_{R,S})}{d} \quad (7)$$

where the subscripts on C represent the species (O or R) and tip and substrate (T or S).

$$C_{O,S} + C_{R,S} = C_O^* \qquad C_{R,T} = C_O^* \quad (8)$$

$$C_{O,S}/C_{R,S} = \theta \quad (9)$$

$$C_{R,S} = C_O^*/(1 + \theta) \qquad C_{R,T} = C_O^* \quad (10)$$

This yields an approximate value for the tip current under feedback conditions as

$$i_T = \frac{nFADC_O^*}{d}\left(\frac{\theta}{1 + \theta}\right) \quad (11)$$

or, since $nFDC_O^* = i_{T,\infty}/4a$ and $A = \pi a^2$, eq 11 can also be written as

$$i_T = \frac{i_{T,\infty}\pi a}{4d}\left(\frac{\theta}{1 + \theta}\right) \quad (12)$$

Equations 11 and 12 thus apply in the zone in Figure 1C. A plot of the approach curve for $\theta = 1$ in this region is shown in Figure 2b.

The overall approach curve current is taken as the sum of eq 6 and eq 11. This total current is shown in Figure 2c. A family of approach curves for different values of θ is shown in Figure 3. Included in this figure is the curve for mass-transfer control to a conductor ($\theta \rightarrow \infty$), given by[2,10]

$$I_T(L) = 0.68 + 0.78377/L + 0.3315 \exp(-1.0672/L) \quad (13)$$

where $L = d/a$ and the dimensionless tip current $I_T = i_T/i_{T,\infty}$. As $\theta \rightarrow 0$, the tip current decreases below that expected for an insulator[2,10]

$$I_T(L) = 1/(0.292 + 1.5151/L + 0.6553 \exp(-2.4035/L)) \quad (14)$$

Figure 4 demonstrates that a comparison of the approximation

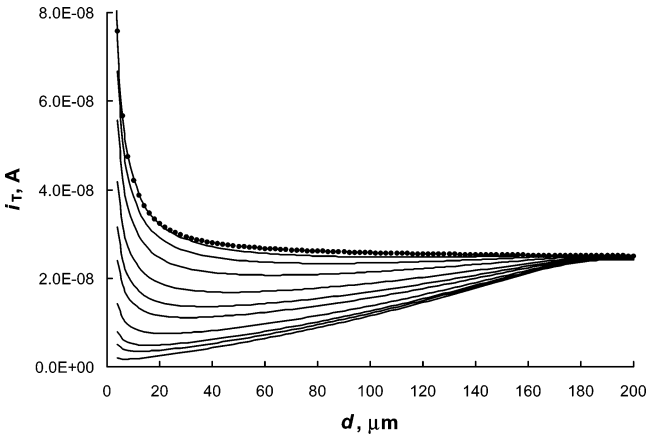

Figure 3. Computed approach curves (equivalent to Figure 2c) for different values of θ. From top to bottom, conductor (solid dots, mass-transfer controlled), eq 13; θ = 8, 4, 2, 1, 0.6, 0.4, 0.2, 0.1, 0.06, and 0.02. Conditions as in Figure 2.

(solid line) used here at large θ and the curve for a conductor (solid dots), eq 13, shows reasonable agreement, considering the relative crudeness of the approximation.

Quasireversible Systems. As for the reversible case, we assume that the tip is initially at a distance d_i from the substrate (at $x = 0$) and is held there for a quiet time τ during which a potential is applied to both tip and substrate. During this time, if the substrate potential E_S is set so that reaction 1 occurs at a finite rate, the concentration gradient that forms there will depend on the heterogeneous rate constants given by the Butler−Volmer relationships for reduction (k_f) and oxidation (k_b)[23]

$$k_f = k^\circ \exp\{-\alpha nF(E - E^{\circ\prime})/RT\} \quad (15)$$

$$k_b = k^\circ \exp\{(1 - \alpha)nF(E - E^{\circ\prime})/RT\} \quad (16)$$

in terms of the standard rate constant k° and the transfer coefficient α, or in terms of θ by making use of eq 2

$$k_f = k^\circ\theta^{-\alpha} \quad \text{and} \quad k_b = k^\circ\theta^{1-\alpha} \quad (17)$$

where it follows that $k_b/k_f = \theta$. The concentration profile that develops at the substrate is, from the Appendix,

$$C_O(x,t) = \frac{C_O^*}{1 + \xi\theta}\left[\xi\theta + \mathrm{erf}\left\{\frac{x}{2(D_Ot)^{1/2}}\right\} + \exp\left\{\frac{k_f}{D_O}(1 + \xi\theta)[x + k_f(1 + \xi\theta)t]\right\}\mathrm{erfc}\left\{\frac{x}{2(D_Ot)^{1/2}} + \frac{k_f}{D_O^{1/2}}(1 + \xi\theta)t^{1/2}\right\}\right] \quad (18)$$

(18) Bard, A. J.; Fan, F.-R. F.; Kwak, J.; Lev, O. *Anal. Chem.* **1989**, *61*, 132.
(19) Bard, A. J.; Denuault, G.; Friesner, R. A.; Dornblaser, B. C.; Tuckerman, L. S. *Anal. Chem.* **1991**, *63*, 1282.
(20) Hubbard, A. T.; Anson, F. C. In *Electroanalytical Chemistry*; Bard, A. J., Ed.; Dekker: New York, 1970; Vol. 4, p 152.
(21) Anderson, L. M.; McDuffie, B.; Reilley, C. N. *J. Electroanal. Chem.* **1966**, *12*, 477.
(22) Anderson, L. M.; Reilley, C. N. *J. Electroanal. Chem.* **1965**, *10*, 295.
(23) Bard, A. J.; Faulkner, L. R. *Electrochemical Methods*; Wiley: New York, 2001; p 96.

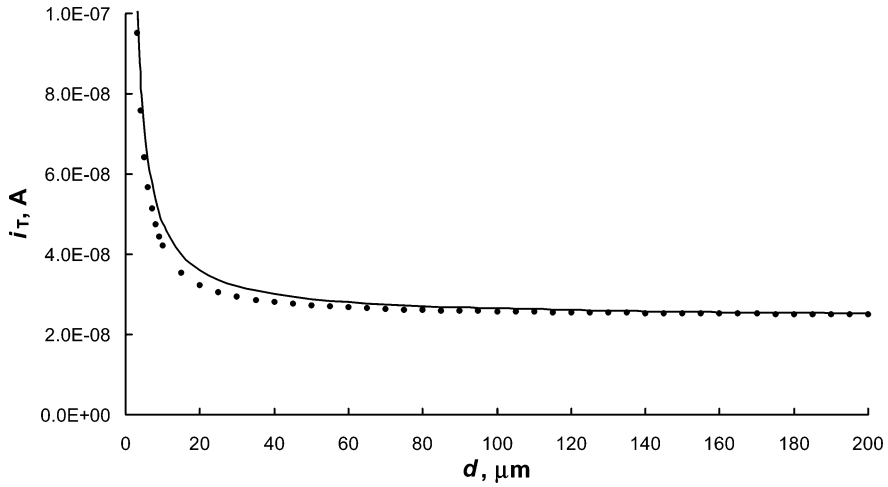

Figure 4. Comparison between computed approach curve (solid line) for $\theta = 1 \times 10^5$ and theoretical curve for mass-transfer control at conductor (solid dots), eq 13. Conditions as in Figure 2.

The tip samples this concentration gradient at a distance $x = d$ at time t, as given by eq 4, so that when written in terms of these parameters, eq 18 leads to an expression for $C_O(d)$. In zones A and B of Figure 1, i_T is then given by eq 6. The concentration profile that the tip samples is then a function of d, $k°$, α, and θ. As $k° \rightarrow \infty$, eq 18, written in terms of d, reduces to eq 5, and i_T given by eq 6 approaches that for the reversible case. As $k° \rightarrow 0$, eq 18 reduces to $C_O(d) = C_O^*$, so that the tip sees an unchanging concentration profile as it approaches the substrate.

For the quasireversible case, the tip feedback current also depends on the magnitude of the oxidation (k_b) and reduction (k_f) rate constants through $k°$, α, and θ, in addition to the tip−substrate separation. The thin-layer cell problem with kinetics has been treated by Anderson and Reilley.[22] Assuming $D_O = D_R = D$ and that E_T is held at a potential where the reduction of O is mass-transfer controlled, using our notation, the tip current can be expressed as

$$i_T = nFAk°\left[C_{R,S}\exp\left\{\frac{(1-\alpha)nF}{RT}(E-E°')\right\} - C_{O,S}\exp\left\{\frac{-\alpha nF}{RT}(E-E°')\right\}\right] \quad (19)$$

where

$$C_{O,S} = i_T d/nFAD \qquad C_{R,S} = C_O^* - C_{O,S} \quad (20)$$

This yields an approximate value for the tip current under feedback conditions as

$$i_T = \frac{nFADC_O^*}{d\left(\frac{D}{k°d\theta^{1-\alpha}} + \frac{1+\theta}{\theta}\right)} = \frac{i_{T,\infty}\pi a}{4d\frac{1+\theta}{\theta}\left(\frac{D\theta^\alpha}{k°d(1+\theta)}+1\right)} = \frac{i_{T,\infty}\pi}{4L\frac{1+\theta}{\theta}\left[\frac{\theta^\alpha}{\Lambda L(1+\theta)}+1\right]} \quad (21)$$

where $\Lambda = ak_s°/D$. As $\Lambda \rightarrow \infty$, eq 21 reduces to eq 12 for the reversible case. More specifically, for reversible feedback to occur, the condition $\theta^\alpha/\Lambda L(1+\theta) \ll 1$ must be met. If the θ limit at both 0 and ∞ are considered, then $\Lambda \gg 1$ is required for reversible feedback to occur. In contrast, for $\Lambda \rightarrow 0$, eq 21 reduces to $i_T = i_{T,\infty}\pi\Lambda\theta^{1-\alpha}/4$ and the feedback current approaches zero. Equation 21 applies in the zone in Figure 1C.

The overall approach curve current is taken as the sum of eqs 6 and 21. For $\Lambda \leq 1$(corresponding to $k° \rightarrow 0$) and $\theta \leq 1$ (for a reduction), the positive feedback current typical of more reversible behavior becomes increasingly less important and blocking of the tip by the substrate becomes increasingly more important. This blocking effect typical of negative feedback is incorporated into eq 6 as shown in eq 22

$$i_T = \frac{4nFD_O aC_O(d)}{1 + (11/10^\Lambda\kappa[(50/\Lambda) - L])} \quad (22)$$

where $\kappa = dk_S°/D$. Equation 22 was found to be important for $0.5 \leq \Lambda \leq 0.05$ and the blocking factor in the denominator was determined by fitting the approximate current found by the sum of eqs 21 and 22 for $L \leq 16$, $0.5 \leq \Lambda \leq 0.05$, and $\theta = 1$, to previously tabulated values.[12] Approach curves for values of the dimensionless kinetic parameter Λ are shown in Figure 5 (solid lines) and compared to previously published tabulated values[12] (solid dots) for $\theta = 1$. Insulating behavior as given by eq 14 is shown as the dotted line and compared to published tabulated values found for $\Lambda = 0.001$ (solid triangles) at $\theta = 1$.

EXPERIMENTAL SECTION

Electrodes. Tip electrodes were either of Au or Pt (CHI Instruments, Austin, TX, RG ~5). The Au ultramicroelectrode (UME) was prepared by sealing nominal 25-μm-diameter Au wire (Goodfellow Metals, Cambridge, England) into glass as previously described[18] and sharpening to a RG of ~10. The substrate electrode was either a 2-mm-diameter Au disk (BAS) or Ir foil (Alfa Aesar) with 6-mm circular diameter exposed to the solution via a Teflon O-ring (McMaster Carr). A Pt wire (Goodfellow Metals) served as the counter electrode and either a saturated Ag/AgCl (CHI Instruments) or saturated SCE (CHI Instruments) as the reference electrode.

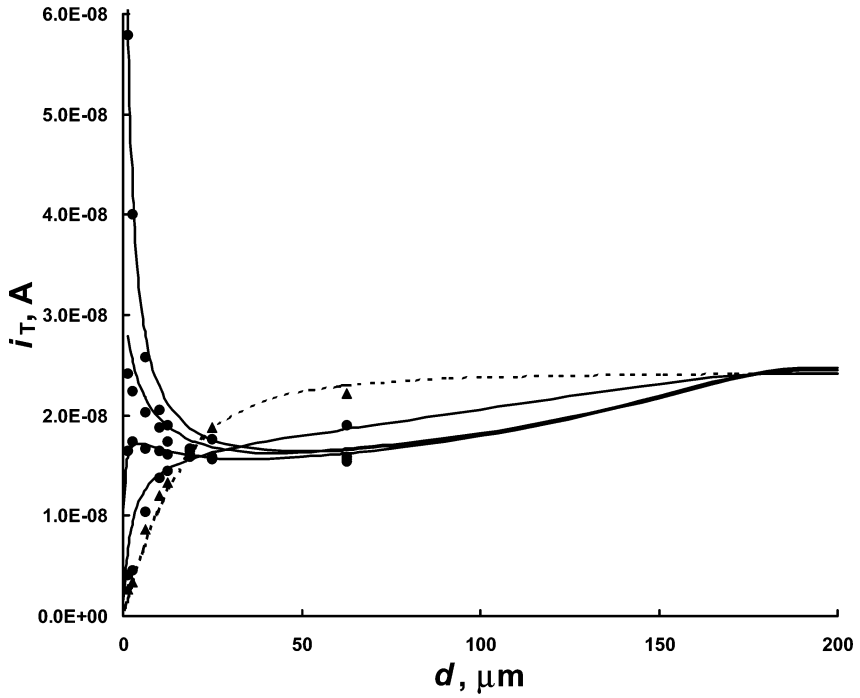

Figure 5. Comparison between computed quasireversible approach curves (solid lines) and published values (solid dots). From top, $\Lambda = 5$, 1, 0.5, and 0.05. The dotted line is the approach curve for an insulator (eq 14) and compared to published data (solid triangles) for $\Lambda = 0.001$. Conditions as in Figure 2 except for $\tau = 0.1$ s and $\mu = 3$ μm/s.

Chemicals. Ferrocenemethanol (FcMeOH), sodium chloride, perchloric acid (70%, redistilled 99.9999%), and sodium perchorate were purchased from Aldrich and used without further purification. Solutions were prepared using MQ treated water (Milli-Q, Millipore). In the experiments with perchloric acid, the solutions were deaerated with argon throughout.

Instrumentation. Cyclic voltammograms and approach curves, tip current, i_T, versus distance, d, were obtained using a CHI900 SECM instrument (CH Instruments). A bipotentiostat configuration was used and the electrochemical cell was Teflon (3-mL capacity).

RESULTS AND DISCUSSION

Approach Curves for Nernstian System. Figure 6 shows experimental approach curves (solid lines) at different potentials for a 1.1 mM FcMeOH solution in 0.1 M NaCl with a 12.5-μm-radius Au tip at an approach speed of 6 μm/s to a 1-mm-radius Au disk after a quiet time, τ, of 5 s and an initial distance, d_i, of 250 μm. The curves show the trends predicted by the approximate theory as functions of θ and traverse behavior showing a high degree of shielding ($\theta = 0.004$) to essentially complete positive feedback ($\theta = 9.6$). A comparison of the experimental approach curves with theory (solid dots) shows good agreement as shown in Figure 6. It is possible that natural convection could be affecting these measurements due to the length of time of the experiment (~45 s) and the movement of the UME tip. However, the good agreement between experiment and theory indicates that these effects are small. The dotted line corresponds to the approach to a conductor as given by eq 13. The inset to Figure 6 shows the steady-state tip voltammogram for the oxidation of FcMeOH. The diffusion-limited plateau is reached at a potential of 0.4 V versus Ag/AgCl, and this potential was used as the tip potential. A diffusion coefficient of 7.1×10^{-6} cm^2/s was calculated from the steady-state limiting current and is in good agreement with that reported by Miao et al. ($D = 7.8 \times 10^{-6}$ cm^2/s).[24] A standard potential of 0.218 V versus Ag/AgCl was measured from the half-wave height of the steady-state voltammogram and is in good agreement with that measured from a cyclic voltammogram (not shown) at the larger Au disk substrate. These values were used in constructing the theoretical curves shown in Figure 6. Note that these curves basically probe the concentration profiles, as was originally carried out with ultramicroelectrodes by Engstrom and co-workers.[7–9] These authors mainly were interested in looking at product distributions and did not probe at sufficiently small distances to find the positive feedback regions.

Approach Curves for Quasi-Reversible System. Experimental (solid lines) and theoretical (solid dots) approach curves are shown in Figure 7 for the oxidation of hydrogen at an Ir substrate in a solution of 0.01 M $HClO_4$ and 0.1 M $NaClO_4$. Hydrogen is produced at a 12.5-μm-radius Pt tip at a constant rate through the reduction $2H^+ + 2e \rightarrow H_2$ by holding the tip at a potential of −0.8 V versus SCE. This represents the diffusion-limited plateau for the reduction of hydrogen ions, as shown in the inset of Figure 7. A half-wave potential of −0.410 V versus SCE was measured at the half-wave height of the steady-state tip voltammogram. The hydrogen generated at the tip electrode has been shown to be oxidized back to H^+ at the substrate at a finite rate when the tip is in close proximity to the substrate.[25] The approach curves were recorded by moving the Pt tip from an initial distance d_i of 173 (top curve) and 181 μm (bottom curve) at a rate of 3 μm/s to a 3-mm-radius Ir foil substrate after a quiet time of 30 s. The shielding increases, and the feedback decreases as predicted, in going from the top curve ($E_S = -0.410$ V vs SCE, $\theta = 1$) to the bottom curve ($E_S = -0.440$ V vs SCE, $\theta =$

(24) Miao, W.; Ding, Z.; Bard, A. J. *J. Phys. Chem. B* **2002**, *106*, 1392.
(25) Zhou, J.; Zu, Y.; Bard, A. J. *J. Electroanal. Chem.* **2000**, *491*, 22.

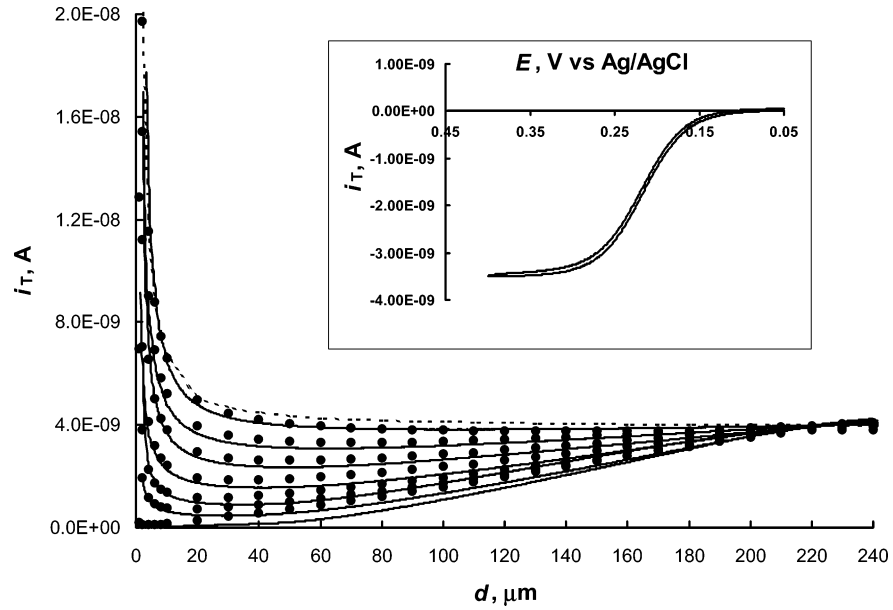

Figure 6. Experimental (solid lines) and theoretical (solid dots) approach curves for 1.1 mM FcMeOH solution in 0.1 M NaCl with a 12.5-μm-radius Au tip at an approach speed of 6 μm/s to a 1-mm-radius Au disk after a quiet time, τ, of 5 s and an initial distance, d_i, of 250 μm. Tip potential was set at 0.4 V vs Ag/AgCl. Values of $D = 7.1 \times 10^{-6}$ cm^2/s and $E^\circ = 0.218$ V vs Ag/AgCl were used in calculating the theoretical approach curves. The dotted approach curve is that for a conductor. Substrate potentials E_S (V vs Ag/AgCl) from top to bottom correspond to 0.160 ($\theta = 9.6$), 0.200 ($\theta = 2.0$), 0.220 ($\theta = 0.93$), 0.240 ($\theta = 0.42$), 0.260 ($\theta = 0.19$), 0.280 ($\theta = 0.090$), and 0.360 V ($\theta = 0.004$). Inset shows voltammogram for oxidation of FcMeOH.

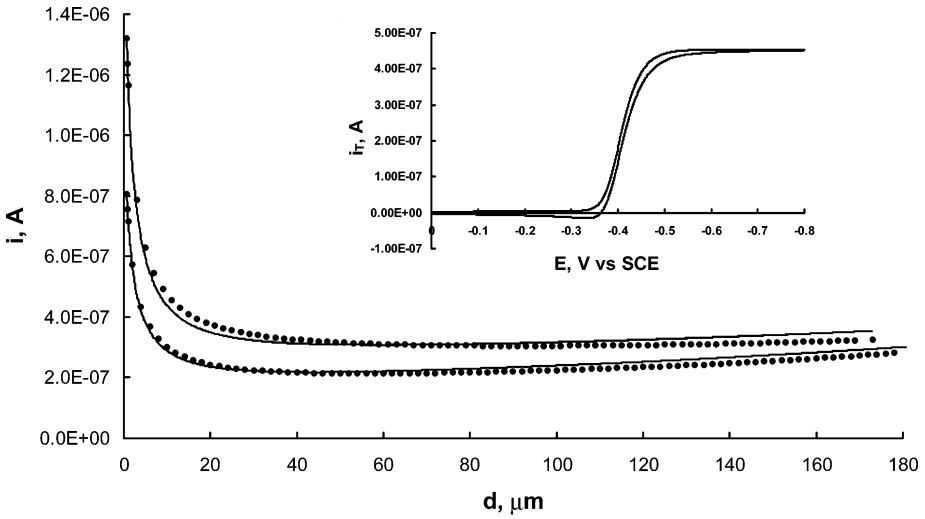

Figure 7. Experimental approach curves (solid lines) and theoretical (solid dots) approach curves for a 0.01 M $HClO_4$ solution in 0.1 M $NaClO_4$ for a 12.5-μm-radius Pt tip at an approach speed of 3 μm/s to a 3-mm-radius Ir foil after a quiet time τ of 30 s and an initial distance, d_i, of 173 (top curve) and 181 μm (bottom curve). The tip potential was set at -0.8 V vs SCE. For theoretical curves, $E^\circ = -0.410$ V vs SCE, $D = 7.10 \times 10^{-5}$ cm^2/s. The top curve corresponds to $E_S = -0.410$ V vs SCE ($\theta = 1$) and was fitted with $k^\circ = 0.20$ cm/s. The bottom curve corresponds to $E_S = -0.440$ V vs SCE ($\theta = 0.31$) and was fitted with $k^\circ = 0.16$ cm/s.

0.31). The experimental approach curves were fitted with the approximate theory using a diffusion coefficient of $D = 7.10 \times 10^{-5}$ cm^2/s,[25] and $k^\circ = 0.20$ cm/s for the $\theta = 1$ curve, and $k^\circ = 0.16$ cm/s for the $\theta = 0.31$ curve. These values are in reasonable agreement with a k° value of 0.25 cm/s determined previously at an Ir substrate.[26]

Determination of Diffusion Coefficients from Approach Curves in Shielding Region. In most SECM approach curves, the current is usually normalized with respect to $i_{T,\infty}$ and the distance with respect to a. These yield dimensionless plots that are independent of D and C_O^*. However in measurements of i_T in the shielding region, the approach curves can be considered "semitransient". That is, although the tip current is essentially at steady state, the concentration profile at the substrate is changing with time. Under these conditions for a Nernstian system, a plot of normalized current, $i_T/i_{T,\infty}$, against d depends on D [for sufficiently small θ (e.g., 0.02−0.14)] (Figure 8). They are independent of C_O^* and n, however. Thus, a fitting of these curves allows one to determine D, without knowledge of other experimental parameters. SECM in this regime shares with other time-of-flight or combined transient and steady-state measurements at an ultramicroelectrode, the ability to extract a value of D without knowledge of C_O^* and n.[27] For example, one can plot

(26) Zoski, C. G. *J. Phys. Chem. B*, submitted.

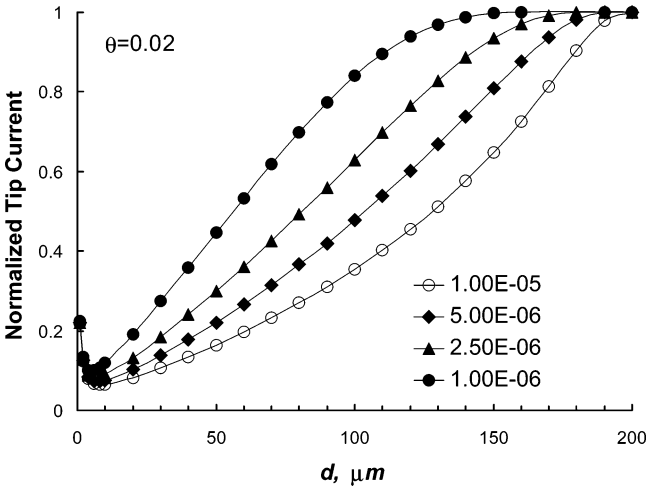

Figure 8. Effect of diffusion coefficient on approach curves. Conditions as in Figure 2, except $\theta = 0.02$, for (left to right) $D = 1 \times 10^{-6}$, 2.5×10^{-6}, 5×10^{-6}, and 1×10^{-5} cm^2/s.

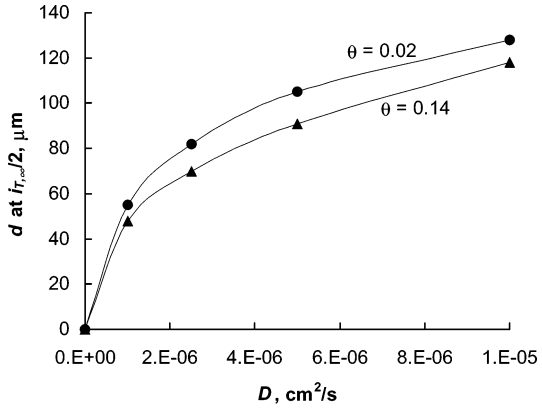

Figure 9. Effect of diffusion coefficient on value of d where $i_T = i_{T,\infty}/2$ for two different values of θ.

the value of d at $i_{T,\infty}/2$, under specified τ, d_i, and θ and correlate that to D, as shown in Figure 9. The good correlation between experiment and approximate theory shown in Figure 6 demonstrates the validity of such an approach.

CONCLUSIONS

The effect of shielding of a UME tip by a larger substrate electrode in SECM has been examined for reversible and quasireversible reactions. The shielding occurs when the potential of the substrate is set so that the substrate reaction is the same as that at the UME tip and the approaching tip then samples the concentration profile setup by the substrate. Within a few micrometers of the substrate, the diffusion layers of the two electrodes interact and it is possible for positive feedback to the tip to occur. An approximate treatment of the shielding effect has been presented and is based on the sum of the currents due to the shielding of the UME tip by the substrate and the feedback that occurs in the resulting thin-layer configuration. For reversible reactions, the shielding effect is a function of the dimensionless potential parameter θ, which is a measure of the substrate potential E_S relative to $E^{\circ\prime}$. For a reduction, when $\theta \gg 1$, approach curves are in good agreement with those for a conductor. For $\theta \leq 1$, the shielding effect causes the tip current to decrease below that expected for an insulator. The good agreement between experimental approach curves at different potentials for a ferrocenemethanol solution with the approximate theory complements the existing theory for reversible (conducting) substrates.

For quasireversible reactions, the effect of shielding of the UME tip by the substrate depends on the value of the standard rate constant k° and the transfer coefficient α in addition to θ for the substrate reaction. For large k°, the i_T versus d curves approach those of a conductor as for reversible kinetics, while for very small k°, insulator behavior is slowly approached. Fitting of the approximate quasireversible theory to experimental approach curves in perchloric acid solutions leads to a rate constant for hydrogen oxidation that is comparable to the fast rate measured in previous studies. Thus, quasireversible shielding in SECM appears to be a novel way of measuring fast kinetics at a substrate surface. Normally, SECM experiments are carried out at substrate potentials where the substrate reaction is opposite to that at the UME tip and the concentration profile at the substrate is unchanging. Under these conditions for fast reactions, this means that there is often a very narrow range of potentials where a rate constant can be determined before the mass-transfer-controlled region is reached. By moving the potential of the substrate into the shielding region (and thereby decreasing k_b at the substrate), the kinetics of the substrate reaction can be effectively slowed and thus more easily measured. Quasireversible shielding may also be useful in reaction-rate imaging, in which the electron-transfer activity of a surface is mapped by SECM. These and further investigations into use of the shielding approach in kinetic investigations are underway in these laboratories.

ACKNOWLEDGMENT

The support of this work by grants from the National Science Foundation [CHE-0109587 (A.J.B.), CHE-0210315 (C.G.Z.)] and the Robert A. Welch Foundation (A.J.B.) is gratefully acknowledged. J.C.A. thanks CONACYT (Mexico) for financial support. We also appreciate the preliminary experiments by Francesco Longobardi on this project.

APPENDIX

Derivation of Eq 18. We begin with the Laplace transform of the concentration profile given as[28]

$$\overline{C_O}(x,s) = \frac{C_O^*}{s} - \frac{k_f C_O^* \exp\{-x(s/D_O)^{1/2}\}}{D_O^{1/2} s(H + s^{1/2})} \qquad \text{(A1)}$$

where s is the Laplace variable and

$$H = \frac{k_f}{D_O^{1/2}} + \frac{k_b}{D_R^{1/2}} = \frac{k_f}{D_O^{1/2}}(1 + \xi\theta) \qquad \text{(A2)}$$

the rate constants k_f (reduction) and k_b (oxidation) are the Butler−Volmer relationships defined in eqs 15 and 16. Laplace inversion

(27) (a) Feldman, B. J.; Feldberg, S. W.; Murray, R. W. *J. Phys. Chem.* **1987**, *91*, 6558. (b) Mosbach, M.; Laurell, T.; Nilsson, J.; Csoregi, E.; Schuhmann, W. *Anal. Chem.* **2001**, *73*, 2468. (c) Denault, G.; Mirkin, M. V.; Bard, A. J. *J. Electroanal. Chem.* **1991**, *308*, 27.

(28) Bard, A. J.; Faulkner, L. R. *Electrochemical Methods*; Wiley: New York, 2001; p 192.

of eq A1[29,30] leads to

$$C_O(x,t) = C_O^* - \frac{k_f C_O^*}{D_O^{1/2} H}\left[\operatorname{erfc}\left\{\frac{x}{2(D_O t)^{1/2}}\right\} - \exp\left\{\frac{x}{D_O^{1/2}}H + H^2 t\right\} \operatorname{erfc}\left\{\frac{x}{2(D_O t)^{1/2}} + Ht^{1/2}\right\}\right] \quad \text{(A3)}$$

In the reversible limit, $k_f \rightarrow \infty$, the exp{} erfc{} term $\rightarrow 0$, and eq A3 simplifies to eq 3 for the concentration profile of a Nernstian system. Similarly, when $x = 0$

$$C_O(0,t) = \frac{C_O^*}{1 + \xi\theta}\left[\xi\theta + \exp\left\{\frac{k_f^2}{D_O} t(1 + \xi\theta) t^{1/2}\right\}\right] \quad \text{(A4)}$$

in agreement with that reported by MacDonald.[31] Substituting for H and k_f in eq A3 leads to eq 18 in the text.

(29) Bard, A. J.; Faulkner, L. R. *Electrochemical Methods*; Wiley: New York, 2001; p 771, Table A1.1.
(30) Oberhettinger, F.; Badii, L. *Tables of Laplace Transforms*; Springer-Verlag: New York, 1973; p 259, eq 5.98.
(31) MacDonald, D. D. *Transient Techniques in Electrochemistry*; Plenum Press: New York, 1977; pp 81−82.

Received for review January 6, 2003. Accepted April 8, 2003.

AC034011X